

# Modelling of coastal long-wave dynamics on unstructured mixed meshes under strong nonlinearity and pronounced baroclinity

Alexey Androsov, Sergey Danilov, Vera Fofonova, Natalja Rakowsky, Karen Helen Wiltshire and Sven Harig

Alfred Wegener Institute, Helmholtz Centre for Polar and Marine Research, Postfach 12-01-61, 27515 Bremerhaven, Germany, (alexey.androsov@awi.de +49(0471) 4831-2106)

## Abstract

Numerical modelling of coastal zone dynamics provides basis for solving a wide range of hydrogeological, engineering and ecological problems. A novel three-dimensional unstructured-mesh model is applied to simulate the dynamics of the density field and turbulence characteristics. The model is based on a finite-volume discretization and works on mixed unstructured meshes composed of triangles and quads. Although triangular meshes are most flexible geometrically, quads are more efficient numerically and do not support spurious inertial modes of triangular cell-vertex discretization. Mixed meshes composed of triangles and quads combine benefits of both. In particular, triangular transitional zones can be used to join quadrilateral meshes of differing resolution. The main aspects of this approach determining its reliability are discussed. The results of several simulations showing the performance of the model with respect to modelling wetting and drying, internal waves, and tidal dynamics are presented.

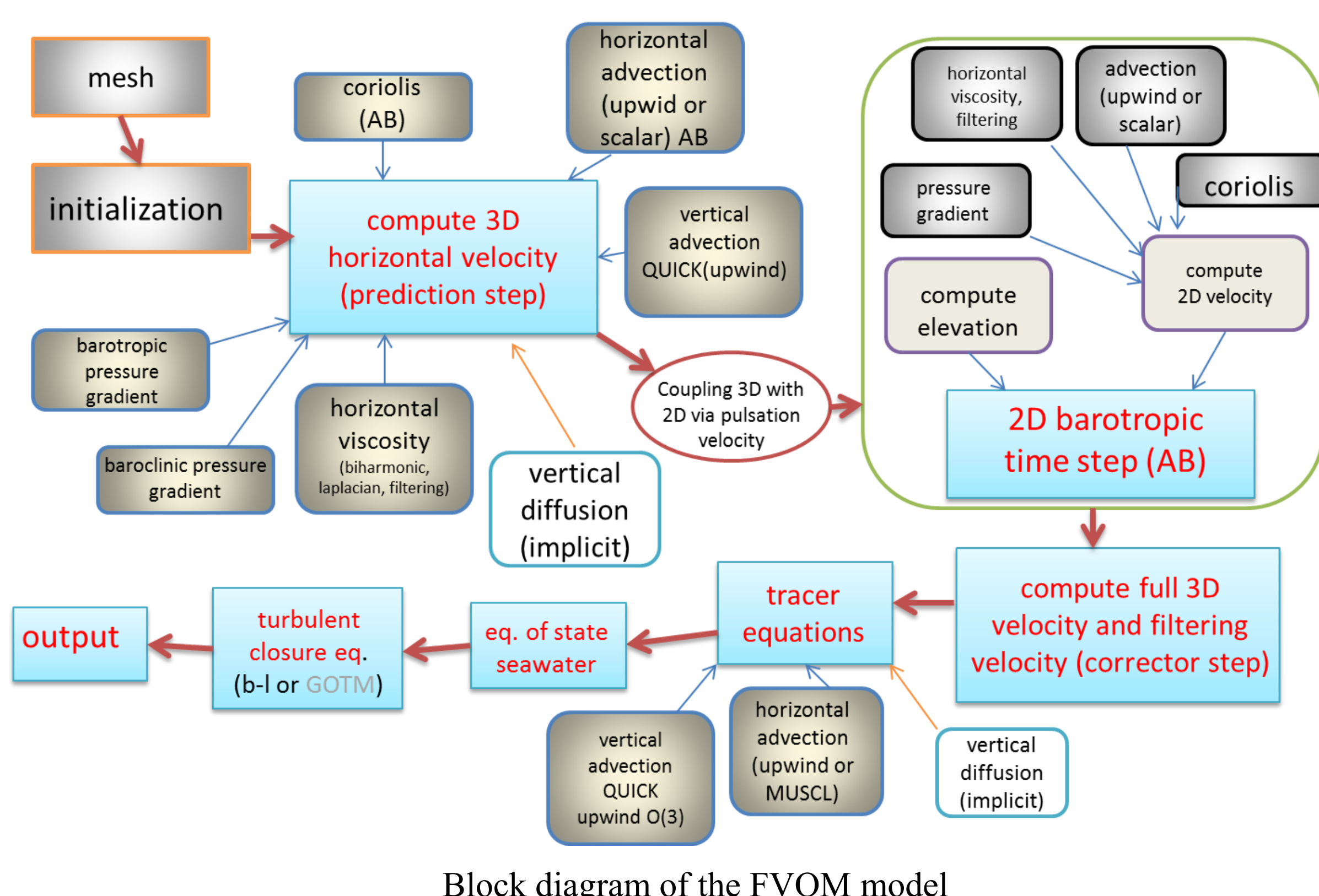
## Strategy of mixed meshes

The advantage of mixed meshes is that quads are more efficient computationally. Indeed, compared to triangular meshes with the same number of scalar degrees of freedom, they have twice less elements and 1.5 times less edges. This leads to shorter cycles and a reduced computational burden. Clearly, in close proximity to coasts one may need the versatility of triangular meshes for geometrical reasons. Outside these areas, the triangular part may only be needed to provide smooth transition between quadrilateral meshes of differing resolution. This is very similar to the idea of nesting, and is perhaps of more value for modeling of large-scale ocean circulation than for applications on the coastal scale.

For many wave applications, the approach may work just fine. However, if nonlinear effects are significant, or, in other words, the grid-scale Reynolds number is sufficiently high, transitional zones may be vulnerable to noise, especially on the triangular part. For this reason, the reliability of mixed meshes depends on whether we are able to control the noise in the case it is generated. That said, it should be clear that the transition we are dealing with here is much more gradual than the jump in resolution in traditional nesting, and fields are always consistent across the coupling zone if dissipation operators are properly adjusted (Danilov and Androsov, 2014).

## Model

- The Finite-Volume Ocean Model (FVOM) model solves three-dimensional primitive equations for the momentum, continuity, density-constituents, and turbulence-characteristics equations.
- FVOM uses a  $\sigma$ -coordinate in the vertical; it is coupled with GOTM turbulence closure sub-model, employs the Smagorinsky formulation for the horizontal viscosity and is equipped with a wetting and drying algorithm.
- FVOM uses a mode-splitting technique to solve the momentum equations with two distinct time steps: external and internal mode time steps to accommodate the faster and slower barotropic and baroclinic responses, respectively.



Block diagram of the FVOM model

## Future developments

- Sediment transport model
- Wind-surge model
- Ice model
- Coupling with global models

## References

- Danilov S. and A. Androsov 2014. Cell-vertex discretization of shallow water equations on mixed meshes. *Ocean Dynamics*. doi: 10.1007/s10236-014-0790-x
- Burchard, H. and K. Bolding, GETM, a general estuarine transport model. Scientific Documentation, European Commission, Report EUR 20253, 157 pp., 2002.
- Burhard H., K. Bolding and M.R. Villarreal. GOTM a general ocean turbulence model. Theory, applications and test cases. Tech. Rep. EUR 18745 EN, European Commission, 1999.

## Results: North Sea barotropic tides

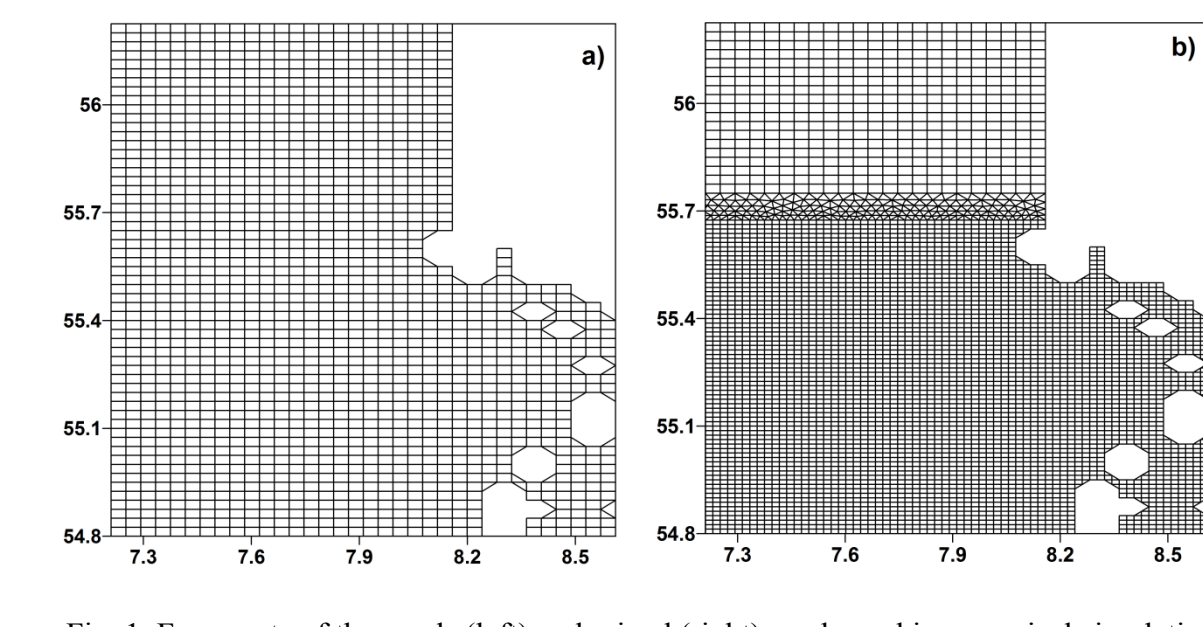


Fig. 1 Fragments of the quads (left) and mixed (right) mesh used in numerical simulations.

Here we present results of simulations of  $M_2$  tide in the North Sea. A large amount of observations is available for this region helping to validate the model. Computations have been performed on three meshes covering the North and Baltic Seas. The first one is composed of triangles (89859 vertices and 168117 cells) with a size varying from 800 m to 5000 m. Two other meshes are derived from a regular mesh covering the area. The second mesh is made of quads, with a small number of triangles added at the coast (153339 vertices, 2252 triangles and 148355 quads) with the cell size of 2500 m. The third grid is a mixed one. It is obtained from the second mesh by nesting into it an area refined by a factor of two through a layer of triangles (180055 vertices, 5089 triangles and 173345 quads), as illustrated in Fig. 1. The third grid illustrates the idea of nesting. Our intention here is only to show that in all cases the algorithm works stable and accurate.

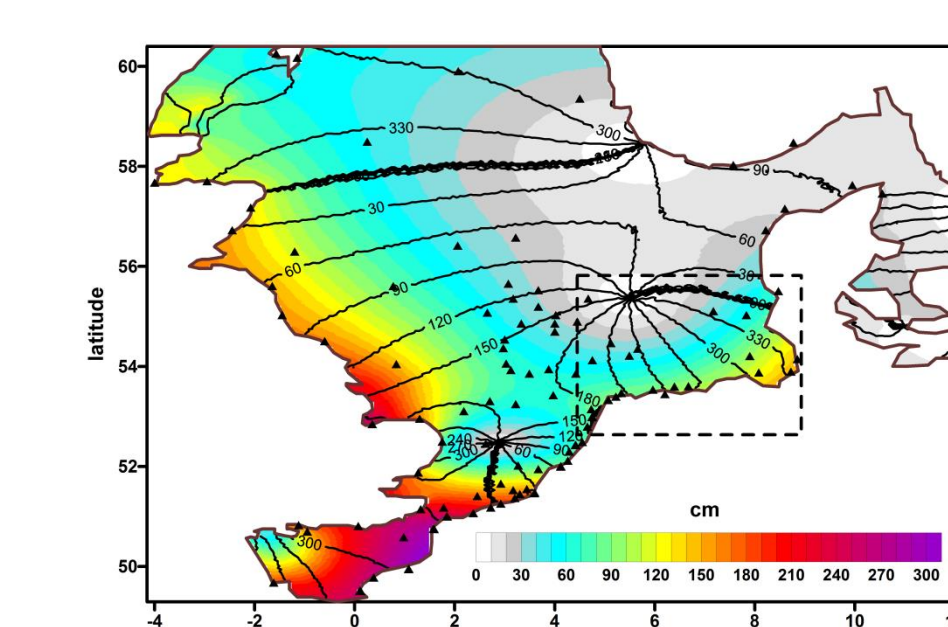


Fig. 2 Tidal map of the  $M_2$  wave: the amplitude in cm and phase (solid line) in degrees. The triangles indicate the station locations. A dashed rectangle shows the domain where the mesh is refined; the transition zone is over its periphery.

The tidal map of  $M_2$  presented in Fig. 2 was obtained on the triangular mesh, and the simulations on the quadrilateral and mixed meshes give very close results, without any tendency to instability or noise on the mixed mesh. Fig. 3 shows the amplitudes and phases computed on different meshes against the observed ones. Some errors seen in the results can be attributed to the uncertainty of bottom topography and the fact that the bottom friction coefficient was taken constant over the whole domain. The RMS error does not exceed 25 cm for all 106 stations for the triangular mesh and makes approximately 20 cm for the rectangular and mixed meshes. Similar results hold also for the stations located inside the dashed region in Fig. 2.

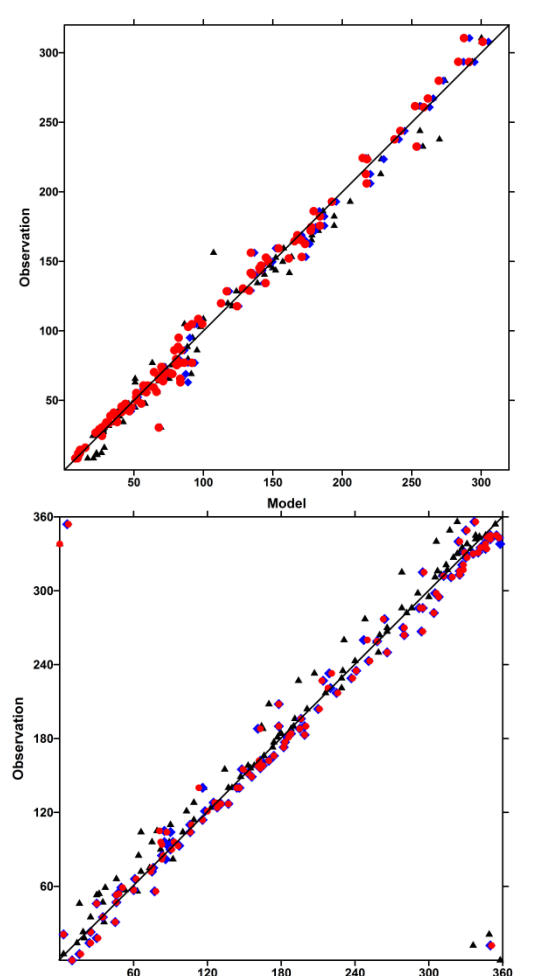


Fig. 3 Comparison of observed and simulated amplitude (upper, cm) and phase (lower, deg). Black triangles, blue rhombi and red circles correspond to the triangular, quadrilateral and mixed meshes respectively.

Somewhat larger RMS error on the triangular mesh can be attributed to the need to suppress the noise as well as to the smaller number of its degrees of freedom.

## Results: Lock Exchange experiment

Lock exchange is simulated in a narrow 3D basin with no rotation. Lock exchange definition: A vertical density front separates waters of different density initially. In the process of adjustment the lighter water moves above the heavier water (Fig. 4). This configuration used a horizontal grid spacing of 2000 m and 40 layers on vertical. Its results agree well with results published in the literature.

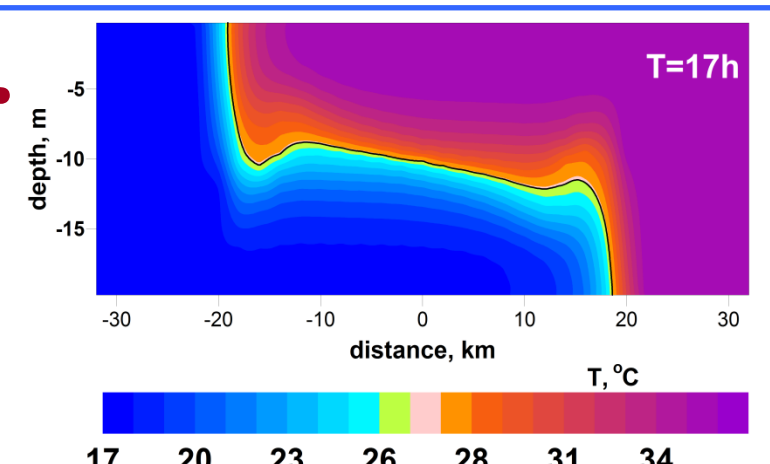


Fig. 4 Simulated temperature after 17 hours of simulation.

## Results: Internal waves

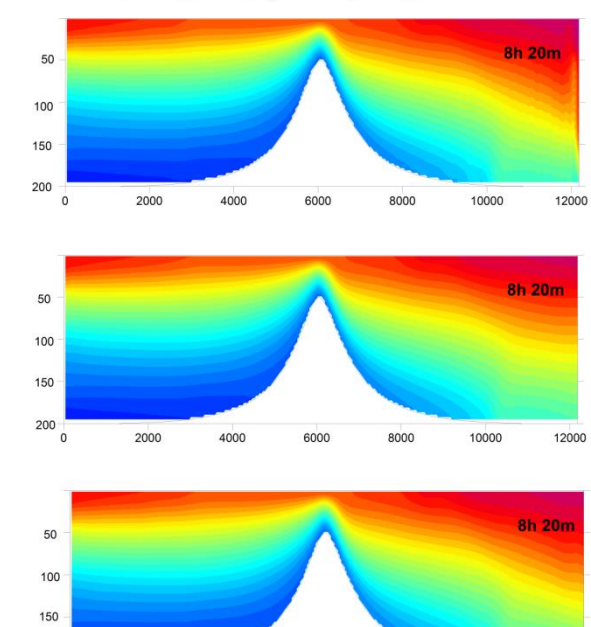


Fig. 5 Solution for three meshes. Upper panel - triangular mesh; middle - quad mesh; bottom - triangular mesh with one layer quads near open boundary.

Statement of boundary conditions on open boundaries for barotropic-baroclinic interaction is a challenging task for coastal applications. This experiment allows us to estimate the efforts necessary for the implementation of coupled conditions for barotropic-baroclinic interaction. The model area is a parallelepiped with two open boundaries and an underwater sill in the center of the area. The horizontal spatial resolution varies from 200 m to 18 m over the sill, and there are 20 sigma layers. On the open boundaries, semidiurnal tide with amplitude 1 cm is imposed in antiphase. The initial temperature is characterized by colder water on the left side of the domain. The relaxation boundary condition is used for temperature. An instability develops close to open boundaries on a fully triangular mesh. One layer quads near the open boundaries eliminates it (Fig. 5). Figure 6 shows the generation of internal wave over a sharp underwater sill.

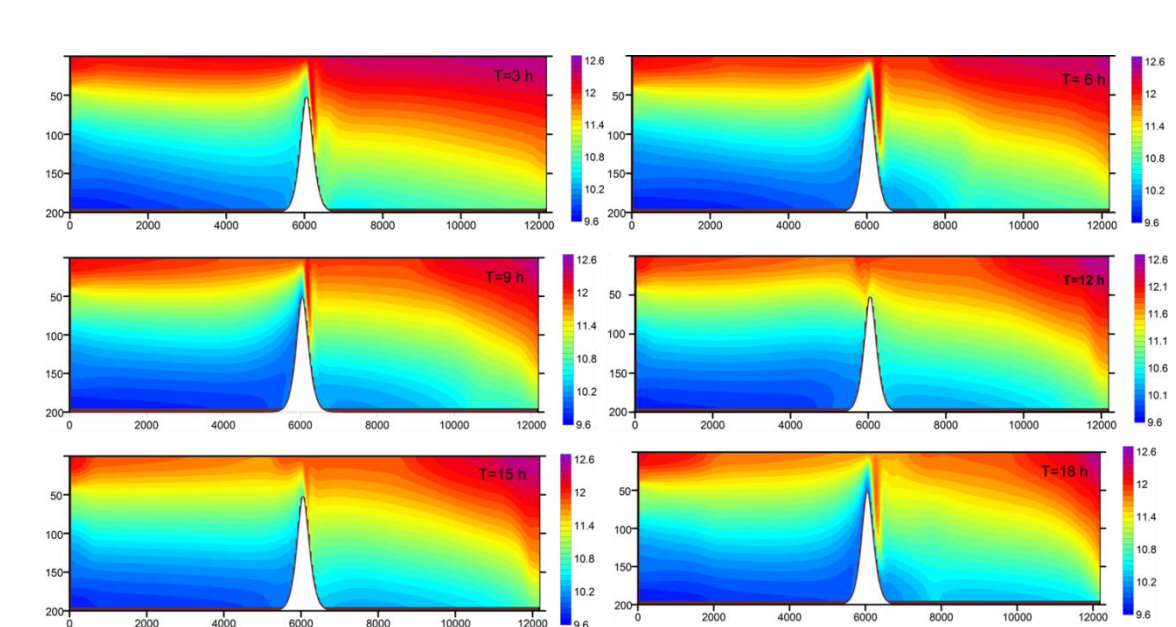


Fig. 6 Time evolution of internal waves over the underwater sill, in the case of sharp bathymetry.

## Results: Sylt-Rømø Bight

In this experiment, the ability of the model to properly simulate the dynamics in complex areas with considerable drying and wetting under tidal motion is demonstrated. The Sylt-Rømø Bight is located in the North Sea between the Danish island Rømø and the German island Sylt (Fig. 7). The main forcing is the  $M_2$  tide with amplitude  $\sim 1$  m (Burchard and Bolding, 2002). Wind forcing and surface heat fluxes are neglected. The turbulence closer model used  $k-\epsilon$  model (GOTM, Burhard et al., 1999).

In Fig. 8, vector plots of average on vertical currents velocities for three phases of the tidal period are shown, during low water, full ebb, and full flood.

The residual currents is shown in Fig. 9. The main features of residual circulation is in very good agreement with GETM model (Burchard and Bolding, 2002). Weak currents in the deep-water channels and intensification of the circulation in the shallow zones are the main features of residual currents in the Sylt-Rømø Bight. Ebb-dominance in the northern part of the Lister Tief channel and flood dominance in the southern part are also present in the residual circulation.

The vertical structure (including wetting and drying features) of the flow and turbulence characteristics are compared with GETM model and shown in Fig. 10 for two points (see Fig. 7).

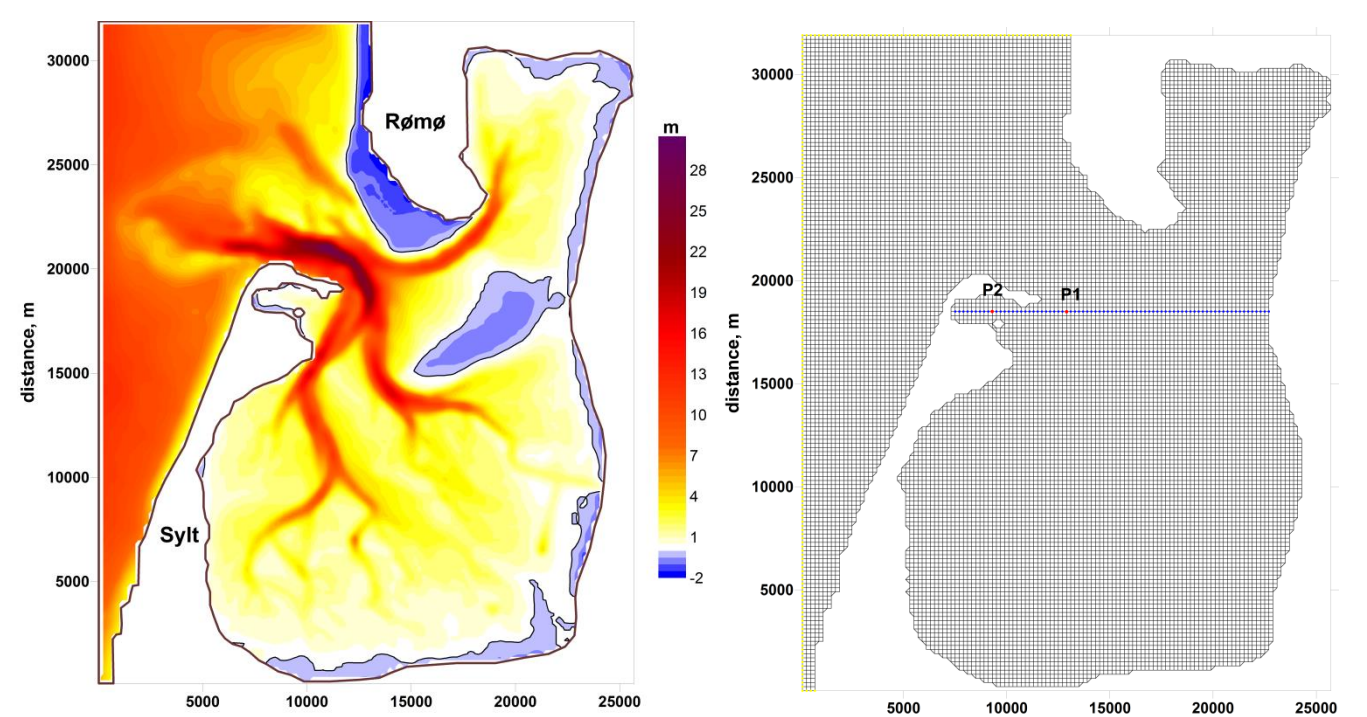


Fig. 7 Bathymetry (left panel) and mesh (left panel) for Sylt-Rømø Bight. The points P1 and P2 show the locations where the temporal evolution of the water column is shown.

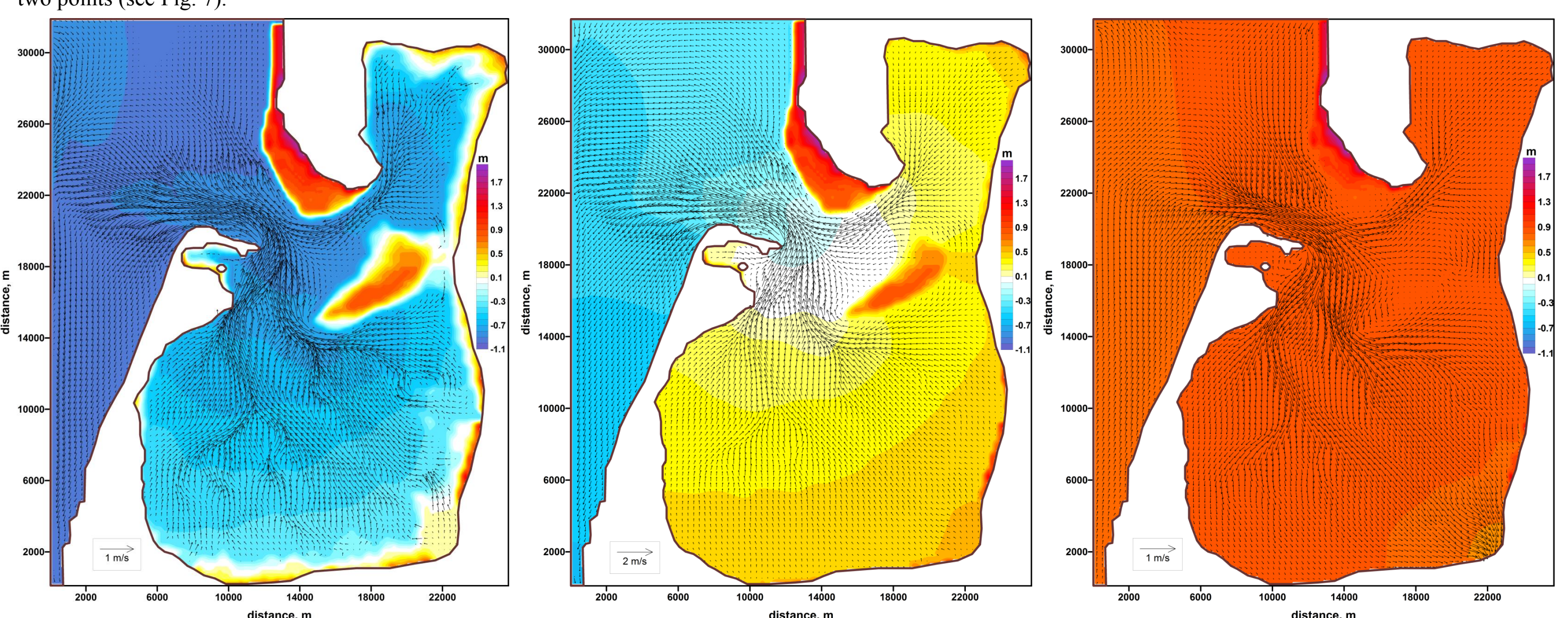


Fig. 8 Vector plots of average on vertical currents velocities. Left panel - low water; middle panel - full ebb; right panel - high water.

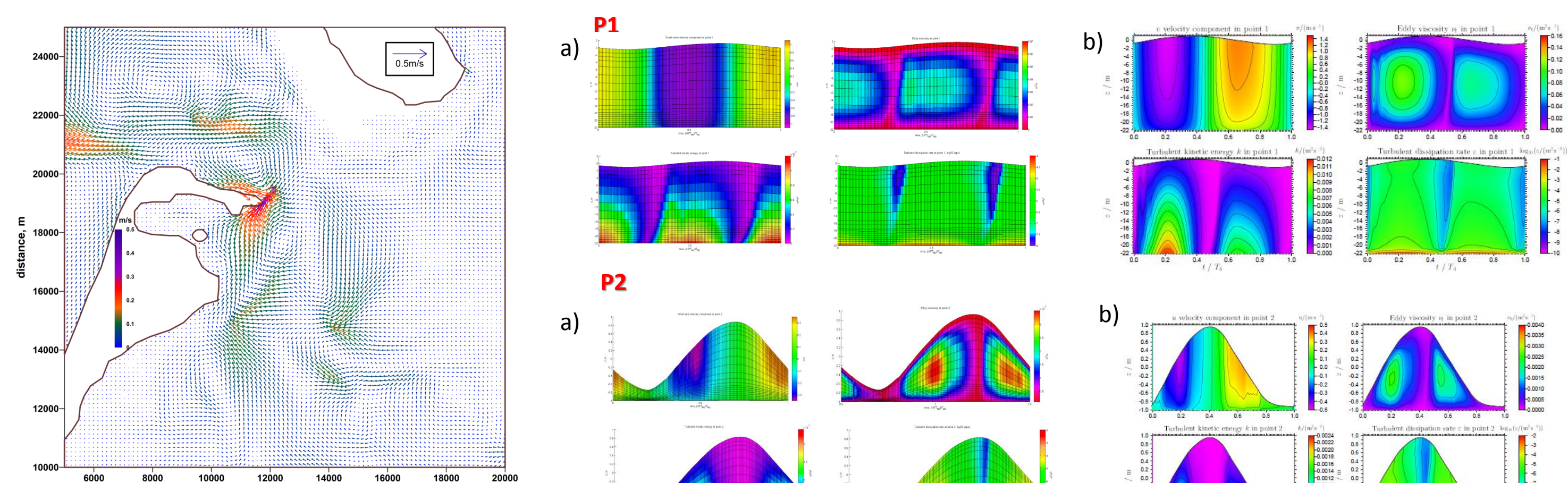


Fig. 9 Residual currents in the Sylt-Rømø Bight.

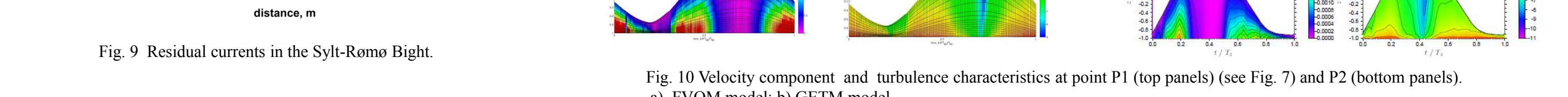


Fig. 10 Velocity component and turbulence characteristics at point P1 (top panels) (see Fig. 7) and P2 (bottom panels). a) FVOM model; b) GETM model.